

# Analyst

Accepted Manuscript

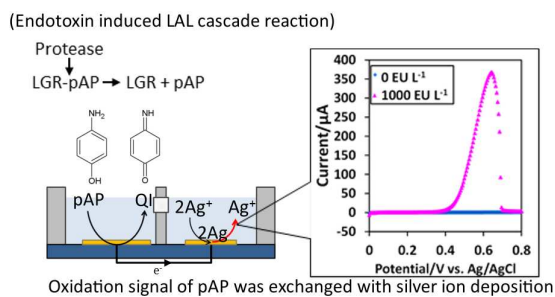


This is an *Accepted Manuscript*, which has been through the Royal Society of Chemistry peer review process and has been accepted for publication.

*Accepted Manuscripts* are published online shortly after acceptance, before technical editing, formatting and proof reading. Using this free service, authors can make their results available to the community, in citable form, before we publish the edited article. We will replace this *Accepted Manuscript* with the edited and formatted *Advance Article* as soon as it is available.

You can find more information about *Accepted Manuscripts* in the [Information for Authors](#).

Please note that technical editing may introduce minor changes to the text and/or graphics, which may alter content. The journal's standard [Terms & Conditions](#) and the [Ethical guidelines](#) still apply. In no event shall the Royal Society of Chemistry be held responsible for any errors or omissions in this *Accepted Manuscript* or any consequences arising from the use of any information it contains.



An extra-highly sensitive sensor for detection of endotoxin was developed. In this sensor, *p*-aminophenole (pAP) was generated with endotoxin induced enzyme reaction and detected with substitutinal stripping voltammetry.

1  
2  
3  
4  
5 **Title**

6  
7 **Electrochemical sensor with substitutional stripping voltammetry for highly**  
8 **sensitive endotoxin assay**  
9  
10

11  
12  
13  
14  
15  
16 **Author's names**

17 **Shinichiro Takano,<sup>1</sup> Kumi Y. Inoue,<sup>\*1,2</sup> Satoko Takahashi,<sup>1</sup> Kosuke Ino,<sup>1</sup> Hitoshi**  
18 **Shiku,<sup>1,3</sup> Tomokazu Matsue,<sup>\*1,2,3</sup>**  
19  
20  
21  
22  
23  
24  
25

26 **Affiliations**

27 **1. Graduate School of Environmental Studies, Tohoku University, 6-6-11-604**  
28 **Aramaki, Aoba, Sendai 980-8579, Japan**

29 **2. Micro System Integration Center, Tohoku University, 6-6-11-604 Aramaki, Aoba,**  
30 **Sendai 980-8579, Japan**

31 **3. Advanced Institute for Materials Research, Tohoku University, 6-6-11-604**  
32 **Aramaki, Aoba, Sendai 980-8579, Japan**  
33  
34  
35  
36  
37  
38  
39  
40  
41  
42  
43  
44

45 **\*Corresponding Authors**

46 **Kumi Y. Inoue**

47 **Phone: +81-22-795-6167, Fax: +81-22-795-6167**

48 **E-mail: inoue@bioinfo.che.tohoku.ac.jp**

49 **Tomokazu Matsue**

50 **Phone: +81-22-795-7209, Fax: +81-22-795-7209**

51 **E-mail: matsue@bioinfo.che.tohoku.ac.jp**  
52  
53  
54  
55  
56  
57  
58  
59  
60

35 **Abstract**

36 We have developed a novel method for detection of endotoxin with extra-high  
37 sensitivity by introducing substitutional stripping voltammetry (SSV). In this method,  
38 *p*-aminophenol (pAP) conjugated peptide (Boc-Leu-Gly-Arg-pAP; LGR-pAP) was used  
39 as a substrate for a protease, which is activated at the last step of the endotoxin-induced  
40 *Limulus* amoebocyte lysate (LAL) cascade reaction. Extra-highly sensitive detection of  
41 pAP liberated by the endotoxin-induced LAL reaction was successfully realized with  
42 SSV based on the accumulation of an amperometric signal owing to exchanging the  
43 oxidation current of pAP generated at an electrode in a reaction cell with silver  
44 deposition on another electrode in a deposition cell. This reaction is driven by the  
45 difference in the redox potential between pAP/quinoneimine and silver/silver ion. The  
46 amount of the deposited silver is quantified by anodic stripping voltammetry (ASV).  
47 This SSV-based endotoxin assay was performed with a chip device comprising two cells,  
48 each of which was connected via a liquid junction made of Vycor<sup>®</sup> glass. The reaction  
49 cell and the deposition cell contained a standard endotoxin sample with LAL reagents  
50 containing LGR-pAP and AgNO<sub>3</sub> solution, respectively. After the cells were electrically  
51 connected for 60 min, ASV was conducted in the deposition cell to quantify the total  
52 electrical charge derived by the oxidation of free pAP in the reaction cell. The ASV

1  
2  
3  
4  
5  
6 53 signal increased with the increase of the endotoxin concentration in the sample solution  
7  
8

9 54 in the range 0.5–1000 EU L<sup>-1</sup>.  
10  
11

12 55  
13

14 56 **Keywords**  
15  
16

17 57 electrochemical biosensor, endotoxin, lipopolysaccharide, *Limulus* amoebocyte lysate  
18  
19

20 58 assay, protease, substitutional stripping voltammetry  
21  
22  
23  
24  
25  
26  
27  
28  
29  
30  
31  
32  
33  
34  
35  
36  
37  
38  
39  
40  
41  
42  
43  
44  
45  
46  
47  
48  
49  
50  
51  
52  
53  
54  
55  
56  
57  
58  
59  
60

1  
2  
3  
4  
5  
6 59 **1. Introduction**  
7  
8

9 Endotoxin is a lipopolysaccharide (LPS) existing on the outer membrane of  
10  
11 Gram-negative bacteria.<sup>1</sup> Although endotoxin itself is chemically stable and thermally  
12  
13 durable, it induces secretion of proinflammatory cytokines leading to septic shock.<sup>2</sup>  
14  
15 Therefore, contamination by endotoxin has been a serious problem for the safety of  
16  
17 medical treatments and medical supplies. The *Limulus* amoebocyte lysate (LAL) assay,  
18  
19 based on the coagulation reaction of hemocytes lysate of horseshoe crabs induced by  
20  
21 endotoxin, is a widely used method to test for endotoxin.<sup>3</sup> The conventional LAL assay  
22  
23 is classified into three major categories called the gel-clotting method, the turbidimetric  
24  
25 method, and the colorimetric method, all of which are based on photometrical detections.  
26  
27  
28  
29  
30  
31  
32  
33  
34  
35  
36  
37  
38  
39  
40  
41  
42  
43  
44  
45  
46  
47  
48  
49  
50  
51  
52  
53  
54  
55  
56  
57  
58  
59  
60

1  
2  
3  
4  
5  
6 77 treatment, particularly in developed countries with increasing incidence of diabetic  
7  
8  
9 78 nephropathy. To overcome the problem of the conventional LAL test, electrochemical  
10  
11  
12 79 techniques have been proposed as promising candidates because they provide  
13  
14  
15 80 easy-to-use, low-cost, and highly sensitive endotoxin sensors.<sup>4</sup> We have previously  
16  
17  
18 81 developed two types of electrochemical sensor based on the LAL reaction.<sup>5-7</sup> One is a  
19  
20  
21 82 LAL-based voltammetric assay for detecting *p*-nitroaniline (pNA) produced from  
22  
23  
24 83 pNA-conjugated peptide (Boc-Leu-Gly-Arg-pNA; LGR-pNA) using differential pulse  
25  
26  
27 84 voltammetry.<sup>5,6</sup> The other is LAL-based amperometric assay using a novel substrate  
28  
29  
30 85 (Boc-Leu-Gly-Arg-*p*-aminophenol; LGR-pAP) specially developed for electrochemical  
31  
32  
33 86 detection.<sup>7</sup> These methods have achieved detection of 10 endotoxin units (EU) per litre  
34  
35  
36 87 within 60 min with easy-to-use chip devices. The sensitivity of these methods is equal  
37  
38  
39 88 to or higher than that of conventional LAL assay; however, there are growing demands  
40  
41  
42 89 for an extra-highly sensitive sensor, particularly among haemodialysis treatment sites.

43  
44 90 In this study, we successfully developed a chip-type endotoxin sensor with  
45  
46  
47 91 extra-high sensitivity by introducing substitutional stripping voltammetry (SSV)<sup>8-11</sup> and  
48  
49  
50 92 using LGR-pAP as a substrate. SSV is based on the accumulation of an amperometric  
51  
52  
53 93 signal by exchanging the redox current to metal deposition. Figure 1A shows the overall  
54  
55  
56 94 scheme of our detection system using SSV. Endotoxins induce the cascade activation of  
57  
58  
59  
60

1  
2  
3  
4  
5  
6 95 zymogens in LAL (Factor C, Factor B and proclotting enzyme), which results in the  
7  
8  
9 96 hydrolysis of LGR-pAP. The enzymatically generated free pAP is oxidized to  
10  
11  
12 97 *p*-quinoneimine (QI) on the reaction electrode, which is electrically connected to the  
13  
14  
15 98 deposition electrode in another cell filled with silver nitrate (AgNO<sub>3</sub>) solution. The  
16  
17  
18 99 resulting oxidation current is exchanged to silver deposition on the deposition electrode  
19  
20  
21 100 (Fig. S1). Similar to a battery cell, this exchange is forced by the difference in the redox  
22  
23  
24 101 potential between pAP/QI and silver/silver ions in separated cells connected by a liquid  
25  
26  
27 102 junction. Unlike pAP, LGR-pAP has no effect of silver deposition, because the potential  
28  
29  
30 103 owing to LGR-pAP oxidation is higher than that from silver ion reduction. Therefore,  
31  
32  
33 104 the amount of the silver deposition corresponds to the concentration of free pAP (Fig  
34  
35  
36 105 S2), which also corresponds to the concentration of endotoxin. The amount of  
37  
38  
39 106 accumulated metallic silver was quantified by high-sensitivity stripping voltammetry.  
40  
41  
42 107 Using this method, 0.5 EU L<sup>-1</sup> of endotoxin was detected within 60 min.  
43

44 108 An additional advantage of this method is the exchange of unstable pAP to  
45  
46  
47 109 stable silver. It is known that pAP loses its electrochemical activity due to air oxidation  
48  
49  
50 110 under neutral and alkaline conditions.<sup>12</sup> The signal exchange from pAP to silver has a  
51  
52  
53 111 potential advantage for extended-time measurement to achieve highly sensitive  
54  
55  
56  
57  
58  
59  
60



1  
2  
3  
4  
5  
6 112 detection. In the future, the combination of SSV with redox cycling of pAP will also  
7  
8  
9 113 increase the sensitivity of the assay.  
10

11 114 In the present study, we first characterized the redox potentials of LGR-pAP,  
12  
13  
14 115 pAP and silver to confirm the strategy to use SSV for endotoxin assay. Then we  
15  
16  
17 116 fabricated a chip device for SSV and demonstrated it to monitor silver deposition by the  
18  
19  
20 117 LAL reaction with and without endotoxin. Silver deposition was observed by  
21  
22  
23 118 monitoring the current flow from the reaction cell and to the deposition cell during  
24  
25  
26 119 silver deposition. Finally, we performed quantitative endotoxin assays with the  
27  
28  
29 120 fabricated device.  
30  
31

32 121

## 33 34 35 122 **2. Material and Methods**

### 36 37 38 123 **2.1. Chemicals and Apparatus**

39  
40 124 An Endospey<sup>®</sup> ES-24S set was purchased from Seikagaku Co. (Japan). This  
41  
42  
43 125 set comprised lyophilized LAL reagents divided into individual test vials and assay  
44  
45  
46 126 buffer. United States Pharmacopeia reference standard endotoxin (USP-RSE) was  
47  
48  
49 127 purchased from Seikagaku Co. (Japan). The USP-RSE was diluted with endotoxin-free  
50  
51  
52 128 water (water for injection, Otsuka Pharmaceutical, Japan) to obtain standard endotoxin  
53  
54  
55 129 solutions. Primary stock solutions prepared in  $2 \times 10^6$  EU L<sup>-1</sup> were stored at  $-80^\circ\text{C}$ .  
56  
57  
58  
59  
60

1  
2  
3  
4  
5  
6 130 Note that EU is a unit expressing endotoxin activity. A secondary stock solution  
7  
8  
9 131 prepared in  $1 \times 10^5$  EU L<sup>-1</sup> was stored at 4°C. According to the protocol for USP-RSE,  
10  
11  
12 132 the stock solutions were mixed by vigorous vortexing for more than 30 min just prior to  
13  
14  
15 133 further dilution. Standard endotoxin solutions for the experiments were prepared  
16  
17  
18 134 immediately before use. LGR-pAP (Watanabe Chemical Industries, Ltd., Japan) and  
19  
20  
21 135 pAP (Wako Pure Chemical Industries, Ltd., Japan) were dissolved in endotoxin-free  
22  
23  
24 136 water to obtain 10 mM stock solutions which were then stored at -20°C. Aqueous  
25  
26  
27 137 solutions were prepared with water for injection. Toxipet endotoxin-free pipet tips  
28  
29  
30 138 (Seikagaku Co., Japan) were used for all endotoxin assays. AgNO<sub>3</sub> was purchased from  
31  
32  
33 139 Wako Pure Chemical Ind., Ltd. (Japan). Poly (dimethylsiloxane) (PDMS, SILPOT 184)  
34  
35  
36 140 was purchased from Dow Corning Toray Co., Ltd. (Japan).

37  
38 141 The cyclic voltammetry (CV) and anodic stripping voltammetry (ASV) were  
39  
40  
41 142 performed with a potentiostat (Compact Stat; Ivium Technologies B.V., The  
42  
43  
44 143 Netherlands). An Ag/AgCl electrode and a Pt plate were used as a reference electrode  
45  
46  
47 144 and a counter electrode, respectively. The CV and the ASV were conducted with a  
48  
49  
50 145 fabricated device using a reaction electrode (5.0 mm in diameter, Au) or a deposition  
51  
52  
53 146 electrode (3.0 mm in diameter, Au) as a working electrode. The reference and counter  
54  
55  
56 147 electrodes were inserted into the solution from above. The deposition current was  
57  
58  
59  
60

1  
2  
3  
4  
5  
6 148 measured with a current amplifier (428-MAN; TFF Corporation Keithley Instruments  
7  
8  
9 149 Inc., Ohio, USA). A data acquisition device (DAQ; NI USB-6211; National Instruments  
10  
11  
12 150 Japan Co., Japan) was inserted between the current amplifier and a monitoring computer  
13  
14  
15 151 in order to control the measurement and data acquisition using a program written in  
16  
17  
18 152 LabVIEW ver. 2010 (National Instruments Japan Co., Japan).

19  
20  
21 153

## 22 23 154 **2.2. Fabrication of the chip device**

24  
25  
26 155 The chip device comprised a glass substrate with patterned electrodes and a  
27  
28  
29 156 PDMS block with two wells to accommodate the solutions (Fig. 1B, C). A glass  
30  
31  
32 157 substrate with patterned electrodes was fabricated by conventional photolithography to  
33  
34  
35 158 make a reaction electrode (Au, 5.0 mm in diameter) and a deposition electrode (Au, 3.0  
36  
37  
38 159 mm in diameter). Titanium, platinum, and gold were successively sputter-deposited  
39  
40  
41 160 (L-332S-FH; Anelva Co., Japan) onto a glass slide (Matsunami Glass Ind., Ltd., Japan)  
42  
43  
44 161 patterned with S1818 positive photoresist (The Dow Chemical Company, USA). After  
45  
46  
47 162 removing the photoresist with acetone (lift-off), an insulation layer was fabricated using  
48  
49  
50 163 a negative photoresist (SU-8 3005; Nippon Kayaku Co., Ltd., Japan). A PDMS block  
51  
52  
53 164 with two wells (7.0 mm in diameter, 5.0 mm in depth) was made as follows. The PDMS  
54  
55  
56 165 pre-polymer was poured into a mould made of acrylic resin and cured in an oven at  
57  
58  
59  
60

1  
2  
3  
4  
5  
6 166 90°C for 30 min. After peeling off the PDMS from the mould, we inserted a Vycor<sup>®</sup>  
7  
8  
9 167 glass rod (3.0 mm in diameter, 3.0 mm in length; Corning, Inc., USA) into a furrow  
10  
11 168 made between the wells. To embed the Vycor<sup>®</sup> glass into the PDMS, PDMS  
12  
13  
14  
15 169 pre-polymer was poured into the furrow, both ends of which were covered with  
16  
17  
18 170 cellophane adhesive tape (Cellotape; Nichiban Co. Ltd., Japan) to prevent the leaking of  
19  
20  
21 171 PDMS into undesired areas. After the PDMS was cured in the oven at 90°C for 30 min,  
22  
23  
24 172 the adhesive tape was removed. The electrode-patterned substrate and the PMDS block  
25  
26  
27 173 were then joined with PDMS.

28  
29  
30 174

### 31 32 175 **2.3. Endotoxin assay using the fabricated device**

33  
34  
35 176 To prepare LAL assay solution containing 1.0 mM LGR-pAP, we put 180  $\mu$ L of  
36  
37  
38 177 assay buffer of Endospecy<sup>®</sup> ES-24S set and 20  $\mu$ L of 10 mM LGR-pAP into one test  
39  
40  
41 178 vial of Endospecy<sup>®</sup> ES-24S set containing lyophilized LAL reagents. Just before the  
42  
43  
44 179 endotoxin assay, the fabricated chip device was treated with O<sub>2</sub> Plasma Asher  
45  
46  
47 180 (LTA-101; Yanaco, Ltd., Japan) at 100 W for 6 min in order to remove the contaminated  
48  
49  
50 181 endotoxin. Next, 130  $\mu$ L of a 1:1 mixture of the LAL assay solution and endotoxin  
51  
52  
53 182 standard solution was placed in the reaction cell of the device. Then, 130  $\mu$ L of 10 mM  
54  
55  
56 183 AgNO<sub>3</sub> with 0.1 M KNO<sub>3</sub> solution was placed in the deposition cell. After the reaction  
57  
58  
59  
60

1  
2  
3  
4  
5  
6 184 cell and the deposition cell were electrically connected, the chip device was incubated at  
7  
8  
9 185 37°C for 60 min. During the incubation, the PDMS well was covered with Parafilm  
10  
11  
12 186 (Pechiney Plastic Packaging, Inc., Chicago, USA) to avoid contamination of the  
13  
14  
15 187 endotoxin and evaporation of the solvent. After the electrical connection was cut, the  
16  
17  
18 188 solution in the deposition cell was exchanged to 130  $\mu\text{L}$  of 0.1 M  $\text{KNO}_3$  solution. The  
19  
20  
21 189 reference electrode and the counter electrode were inserted into the deposition cell to  
22  
23  
24 190 perform ASV using the deposition electrode as the working electrode. The scan rate for  
25  
26  
27 191 ASV was set to 20  $\text{mV s}^{-1}$  to improve its productivity and accuracy.<sup>9</sup> From the ASV  
28  
29  
30 192 voltammogram, the total electrical charge ( $Q$ ) was calculated with following equation:

31  
32 193 
$$Q = \int I dt, \quad (1)$$
  
33  
34

35 194 where  $I$  is the current observed on ASV,  $t$  is the elapsed time from the start of the ASV  
36  
37  
38 195 measurement, and  $Q$  is the total electrical charge produced by oxidation at the reaction  
39  
40  
41 196 electrode while it was connected to the deposition electrode.  
42  
43  
44 197

### 45 46 198 **3. Results and Discussion**

#### 47 48 49 199 **3.1 Comparison of formal redox potential of pAP, LGR-pAP, and $\text{AgNO}_3$ solution**

50  
51  
52 200 As mentioned in the introduction, the driving force of the deposition step of  
53  
54  
55 201 SSV is the potential difference between the reaction electrode and the deposition  
56  
57  
58  
59  
60

1  
2  
3  
4  
5  
6 202 electrode. Therefore, we first checked the formal redox potential of LGR-pAP, pAP and  
7  
8  
9 203 silver in the deposition system using cyclic voltammetry. Figure 2A shows cyclic  
10  
11  
12 204 voltammograms of 1.0 mM LGR-pAP and 1.0 mM pAP solutions in ES-24S assay  
13  
14  
15 205 buffer using the reaction electrode as a working electrode. The scan rate was  $20 \text{ mVs}^{-1}$ .  
16  
17  
18 206 As a reference, a cyclic voltammogram of the assay buffer is also shown in the same  
19  
20  
21 207 graph. Peaks shown around  $-0.30 \text{ V}$  indicate the reduction of dissolved oxygen in the  
22  
23  
24 208 solutions. When the potential of the Au working electrode was scanned upward from  $0.0$   
25  
26  
27 209  $\text{V}$ , LGR-pAP began to be oxidized at  $+0.35 \text{ V}$ . The oxidation current reached a peak at  
28  
29  
30 210  $+0.47 \text{ V}$ , and no obvious reduction current of the oxidized LGR-pAP was observed on  
31  
32  
33 211 the reversed potential sweep from  $+0.80 \text{ V}$  to  $-0.60 \text{ V}$ . The reason for missing the  
34  
35  
36 212 reduction current, which was clearly observed in our previous paper<sup>7</sup>, was due to the  
37  
38  
39 213 difference in reactivity of the substrate. The reduction of the oxidized LGR-pAP in the  
40  
41  
42 214 reversed scan was difficult at the Au surface in the present potential range compared  
43  
44  
45 215 with that at the carbon surface in the previous paper. On the other hands, pAP showed  
46  
47  
48 216 clear oxidation and reduction peaks at  $+0.12 \text{ V}$  and  $-0.06 \text{ V}$ , respectively. This indicates  
49  
50  
51 217 a reversible reaction of pAP/QI redox couple. The formal redox potential of pAP/QI  
52  
53  
54 218 was estimated to be  $+0.03 \text{ V}$  from this result. Figure 2B shows a cyclic voltammogram  
55  
56  
57 219 of  $10 \text{ mM AgNO}_3$  in  $100 \text{ mM KNO}_3$  solution using the deposition electrode as a  
58  
59  
60

1  
2  
3  
4  
5  
6 220 working electrode. When the potential of the working electrode was scanned downward  
7  
8  
9 221 from +0.80 V, silver ions began to be reduced to silver at +0.39 V. On the reverse sweep,  
10  
11  
12 222 the deposited silver on the electrode was oxidized back to silver ions at +0.39 V. No  
13  
14  
15 223 obvious redox current was observed above +0.65 V. This means that the deposited silver  
16  
17  
18 224 was completely stripped away during the potential scan from +0.39 V to +0.65 V.  
19  
20  
21 225 Importantly, Fig. 2B indicates that the deposition of silver begins at +0.39 V. Therefore,  
22  
23  
24 226 LGR-pAP, of which oxidation begins at +0.35 V, cannot promote silver deposition in the  
25  
26  
27 227 deposition step, while pAP, of which oxidation begins above +0.03 V, promotes the  
28  
29  
30 228 silver deposition. These results indicate the possibility to use LGR-pAP as an LAL  
31  
32  
33 229 substrate for endotoxin detection with SSV.  
34  
35  
36  
37  
38  
39  
40  
41  
42  
43  
44  
45  
46  
47  
48  
49  
50  
51  
52  
53  
54  
55  
56  
57  
58  
59  
60

230

### 231 **3.2 Measurement of deposition current**

232 To confirm the strategy of LAL-based SSV endotoxin detection using  
233 LGR-pAP, the current in the deposition process was measured using the current  
234 amplifier connected to the reaction electrode and the deposition electrode. The mixture  
235 solution containing the LAL reagent, 0.5 mM LGR-pAP, and endotoxin was put into the  
236 reaction cell, and 10 mM of AgNO<sub>3</sub> was put into the deposition cell. The recording of  
237 the current was started a few minutes before the electrical connection between the

1  
2  
3  
4  
5  
6 238 reaction and deposition cell. After putting the device covered with the Parafilm into the  
7  
8  
9 239 incubator which was maintained at 37°C, we connected the cells through the current  
10  
11  
12 240 amplifier. It takes less than 3 min to start the recording from the mixing of the endotoxin  
13  
14  
15 241 and reagents. Figure 3A shows a comparison of the deposition current with and without  
16  
17  
18 242 endotoxin. The arrow shows the time to connect the cells. When the reaction mixture  
19  
20  
21 243 contained 1000 EU L<sup>-1</sup> endotoxin, the deposition current increased rapidly about 20 min  
22  
23  
24 244 after mixing the endotoxin and reagents. In contrast, no obvious increase of the  
25  
26  
27 245 deposition current was observed without endotoxin. These results indicate that the most  
28  
29  
30 246 of the deposition current is induced by endotoxin activating the LAL reaction to release  
31  
32  
33 247 free pAP. After measuring the deposition currents, the amount of silver deposited on the  
34  
35  
36 248 deposition electrode was measured with ASV (Fig. 3B) at a scan rate was 20 mV s<sup>-1</sup>. A  
37  
38  
39 249 characteristic peak of silver stripping was observed when the sample containing 1000  
40  
41  
42 250 EU L<sup>-1</sup> endotoxin was tested. The stripped amount of silver was calculated to be 3616  
43  
44  
45 251 μC, which was consistent of the deposited amount of silver ions calculated from the  
46  
47  
48 252 result shown in Fig. 3A (4126 μC). In contrast, only a small stripping peak was  
49  
50  
51 253 observed when the reaction mixture without endotoxin was tested. These results also  
52  
53  
54 254 indicate the consistency of our strategy of LAL-based SSV endotoxin detection using  
55  
56  
57 255 LGR-pAP.  
58  
59  
60



1  
2  
3  
4  
5  
6 256  
7  
8

9 257 **3.3 Quantitative endotoxin assay with SSV using the fabricated device**

10  
11 258 Quantitative endotoxin detection with SSV was performed using the fabricated  
12  
13  
14 259 chip device. The reaction cell containing LAL reagent, 0.5 mM LGR-pAP, and 0–1000  
15  
16  
17 260 EU L<sup>-1</sup> endotoxin was electrically connected to the deposition cell containing 10 mM  
18  
19  
20 261 AgNO<sub>3</sub> for 60 min. After disconnecting from the reaction cell, the deposition cell was  
21  
22  
23 262 filled with new 0.1 M KNO<sub>3</sub> solution for ASV. Figure 4A shows the results of ASV with  
24  
25  
26 263 different concentrations of endotoxin. The oxidation currents in ASV increased with the  
27  
28  
29 264 concentration of endotoxin, indicating that this oxidation response resulted from  
30  
31  
32 265 stripping the silver deposited via oxidation of pAP released by the endotoxin-induced  
33  
34  
35 266 LAL reaction. Multiple peaks observed in the voltammograms of 0.1–100 EU L<sup>-1</sup> were  
36  
37  
38 267 caused by the difference in the bonding force “between the electrode and deposited  
39  
40  
41 268 metals (E-M bond)” and “between atoms of deposited metals (M-M bond)”.<sup>13, 14</sup> The  
42  
43  
44 269 stronger E-M bond dissociates at a higher potential than does the weaker M-M bond.  
45  
46  
47 270 Figure 4B shows the calibration plot for the quantitative endotoxin assay based on the  
48  
49  
50 271 total electrical charge of the ASV response calculated by Eq. (1). Each point  
51  
52  
53 272 corresponds to the mean value, and error bars indicate the standard deviation obtained  
54  
55  
56 273 from independent measurements. Electrical charges increased with the increase in  
57  
58  
59  
60

1  
2  
3  
4  
5  
6 274 endotoxin concentration in the range of 0.1–1000 EU L<sup>-1</sup>. The shape of calibration  
7  
8  
9 275 curve was not linear because the LAL reaction is a cascade reaction constructed with  
10  
11  
12 276 multiple proenzyme activated in order. The cascade reaction makes the progress of LAL  
13  
14  
15 277 reaction to follow the sigmoidal curve with time and also causes the nonlinear  
16  
17  
18 278 relationship between the current values and LPS concentrations at a given time point.  
19  
20  
21 279 The detection limits (adapting 3σ of the blank) and minimum limit of determination  
22  
23  
24 280 (adapting 10σ of the blank) of this study were 0.5 EU L<sup>-1</sup> and 100 EU L<sup>-1</sup>, respectively,  
25  
26  
27 281 calculated by the IUPAC recommended methods<sup>15</sup>. The limit of determination would  
28  
29  
30 282 have been improved if more detailed test had been performed at the range of 10 EU L<sup>-1</sup>  
31  
32  
33 283 and 100 EU L<sup>-1</sup>. The measurement range was 0.5-1000 EU L<sup>-1</sup>. Compared with our  
34  
35  
36 284 previous study<sup>7</sup>, the detection limit was improved from 10 EU L<sup>-1</sup> to 0.5 EU L<sup>-1</sup> on  
37  
38  
39 285 using the chip type device. With the improvement of the detection limit, the  
40  
41  
42 286 measurement range was widened from 10-1000 EU L<sup>-1</sup> to 0.5-1000 EU L<sup>-1</sup>. This range  
43  
44  
45 287 satisfactorily covers endotoxin levels of less than 30 EU L<sup>-1</sup>, which is defined as  
46  
47  
48 288 ultrapure dialysis water by the Associated for the Advancement of Medical  
49  
50  
51 289 Instrumentation (AAMI). Considering the fact that the detection limit of commonly  
52  
53  
54 290 used LAL reagent is 30 EU L<sup>-1</sup>,<sup>16</sup> our novel method innovatively improves endotoxin  
55  
56  
57 291 assay. We should emphasize that our system ensures the safety of long-term dialysis  
58  
59  
60

1  
2  
3  
4  
5  
6 292 patients by meeting the stricter standard (less than 1 EU L<sup>-1</sup>) for ultrapure dialysis fluid  
7  
8  
9 293 defined by The Japanese Society for Dialysis Therapy<sup>17</sup> within 60 min with a small  
10  
11  
12 294 device applicable to the onsite monitoring. Higher sensitivity will be available by taking  
13  
14  
15 295 longer connection time because the longer connecting time is, the more LAL reaction  
16  
17  
18 296 progresses as well as the more Ag deposits (Fig. S3), resulting in the larger ASV signal.  
19  
20  
21 297 As the presented method involves a trade-off between the sensitivity and detection time,  
22  
23  
24 298 the selection of the optimal detection time should be considered in the practical use by  
25  
26  
27 299 taking the required detection limit and allowed detection time into account.  
28

29  
30  
31 300

#### 32 301 **4. Conclusions**

33  
34  
35 302 In this study, we developed a novel endotoxin detection method based on LAL  
36  
37  
38 303 assay and SSV. In this method, the generation of free pAP by endotoxin-induced LAL  
39  
40  
41 304 reaction is substituted to the integration of silver deposition which is then quantified by  
42  
43  
44 305 ASV. First, we checked the redox potential of LGR-pAP, pAP and silver using cyclic  
45  
46  
47 306 voltammetry in order to estimate the driving force of the deposition step in SSV. The  
48  
49  
50 307 result showed that pAP, of which oxidation begins above +0.03 V, promotes the silver  
51  
52  
53 308 deposition beginning below +0.39 V, while LGR-pAP, of which oxidation begins above  
54  
55  
56 309 +0.35 V, does not promote the silver deposition in the deposition step. Then, we  
57  
58  
59  
60

1  
2  
3  
4  
5  
6 310 measured the current in the deposition process on the fabricated chip device to ensure  
7  
8  
9 311 the strategy of LAL-based SSV endotoxin detection. The deposition current was  
10  
11  
12 312 observed only when the reaction mixture contained endotoxin. The total charge  
13  
14  
15 313 observed in the detection process was consistent of the charge observed in the  
16  
17  
18 314 subsequent stripping process.

19  
20  
21 315 Finally, we performed quantitative endotoxin assays using the fabricated chip  
22  
23  
24 316 device. The electrical charges obtained from the silver stripping current increased with  
25  
26  
27 317 the concentration of endotoxin in the solution. The detection limit was 0.5 EU L<sup>-1</sup> for a  
28  
29  
30 318 LAL reaction time of 60 min. This method will provide simple quantitative analysis  
31  
32  
33 319 tools for extra-low-concentration endotoxin in dialysis water and on medical  
34  
35  
36 320 instruments.

37  
38  
39  
40  
41 321

## 42 322 **Acknowledgements**

43  
44 323 This research was supported by Grant-in-Aid for Young Scientists (B) (No.  
45  
46  
47 324 23750073) from the Japan Society for the Promotion of Science (JSPS), and the  
48  
49  
50 325 Supporting Industry Project of the Ministry of Economy, Trade and Industry. It was also  
51  
52  
53 326 partly supported by a Grant-in-Aid for Scientific Research (A) (No. 22245011) from  
54  
55  
56 327 JSPS, and by Special Coordination Funds for Promoting Science and Technology,  
57  
58  
59  
60

1  
2  
3  
4  
5  
6 328 Creation of Innovation Centres for Advanced Interdisciplinary Research Areas Program  
7  
8

9 329 from the Japan Science and Technology Agency.  
10  
11  
12  
13  
14  
15  
16  
17  
18  
19  
20  
21  
22  
23  
24  
25  
26  
27  
28  
29  
30  
31  
32  
33  
34  
35  
36  
37  
38  
39  
40  
41  
42  
43  
44  
45  
46  
47  
48  
49  
50  
51  
52  
53  
54  
55  
56  
57  
58  
59  
60

330 **References**

- 331 1 E. T. Rietschel, T. Kirikae, F. U. Schade, U. Mamat, G. Schmidt, H. Loppnow, A. J.  
332 Ulmer, U. Zähringer, U. Seydel, F. D. Padova, M. Schreier and H. Brade, *FASEB J.*,  
333 1994, **8**, 217–225.
- 334 2 R. B. Yang, M. R. Mark, A. Gray, A. Huang, M. H. Xie, M. Zhang, A. Goddard, W. I.  
335 Wood, A. L. Gurney and P. J. Godowski, *Nature*, 1998, **395**, 284–288.
- 336 3 S. Iwanaga, *Proc. Jpn. Acad. Ser. B*, 2007, **83**, 110–119.
- 337 4 P. Miao, *RSC Adv.*, 2013, **3**, 9606–9617.
- 338 5 K. Y. Inoue, K. Ino, H. Shiku and T. Matsue, *Electrochem. Commun.*, 2010, **12**,  
339 1066–1069.
- 340 6 K. Y. Inoue, S. Takahashi, K. Ino, H. Shiku and T. Matsue, *Innate Immun.*, 2011, **18**,  
341 343–349.
- 342 7 K. Y. Inoue, S. Takano, S. Takahashi, Y. Ishida, K. Ino, H. Shiku and T. Matsue,  
343 *Analyst*, 2013, **138**, 6523 – 6531.
- 344 8 T. Horiuchi, O. Niwa, M. Morita and H. Tabei, *Anal. Chem.*, 1992, **64**, 3206–3208.
- 345 9 T. Horiuchi, O. Niwa and H. Tabei, *Anal. Chem.*, 1994, **66**, 1224–1230.
- 346 10 M. Morita, O. Niwa and T. Horiuchi, *Electrochim. Acta*, 1997, **42**, 3177–3183.

- 1  
2  
3  
4  
5  
6 347 11 T. Yasukawa, Y. Yoshimoto, T. Goto and F. Mizutani, *Biosens. Bioelectron.*, 2012,  
7  
8  
9 348 **37**, 19–23.  
10  
11  
12 349 12 E. P. Gil, H. T. Tang, H. B. Halsall, W. R. Heineman and A. S. Misiego, *Clin.*  
13  
14  
15 350 *Chem.*, 1990, **36**, 662–665.  
16  
17  
18 351 13 S. P. Perone, *Anal. Chem.*, 1963, **35**, 2091–2094.  
19  
20  
21 352 14 M. M. Nicholson, *Anal. Chem.*, 1960, **32**, 1058–1062.  
22  
23  
24 353 15 IUPAC ANALYTICAL CHEMISTRY DIVISION, *Spectrochim. Acta B*, 1978, **33**,  
25  
26 354 241-246.  
27  
28  
29 355 16 J. Bommer and B. L. Jabert, *Semin. Dial.*, 2006, **19**, 115–119.  
30  
31  
32 356 17 I. Masakane, Y. Tubakihara, T. Akiba, Y. Watanabe and K. Iseki, *Ther. Apher. Dial.*,  
33  
34  
35 357 2008, **12**, 457–463.  
36  
37  
38 358  
39  
40  
41 359  
42  
43  
44 360  
45  
46  
47 361  
48  
49  
50 362  
51  
52  
53 363  
54  
55  
56 364  
57  
58  
59  
60

1  
2  
3  
4  
5  
6 365 **Figure Captions**  
7  
8

9 366

10  
11 367 **Figure 1.** (A) Principle of the LAL-based SSV endotoxin assay. (B) Photograph of the  
12  
13 chip device. (C) Diagram of the chip device structure.  
14  
15 368  
16  
17 369

18  
19  
20 370 **Figure 2.** (A) Cyclic voltammograms of assay buffer, 1.0 mM LGR-pAP, and 1.0 mM  
21  
22 pAP obtained with the reaction electrode on the chip device. LGR-pAP and pAP were  
23  
24 371  
25  
26 372 dissolved in the assay buffer. (B) Cyclic voltammogram of 10 mM AgNO<sub>3</sub> in 100 mM  
27  
28 KNO<sub>3</sub> obtained with the deposition electrode on the chip device. Potentials were swept  
29  
30 373  
31  
32 374 upward from 0.0 V Fig. A and downward from +0.8V in Fig. B at a scan rate 20 mVs<sup>-1</sup>.  
33  
34

35 375

36  
37  
38 376 **Figure 3.** (A) Deposition currents observed with 1000 EU L<sup>-1</sup> and without endotoxin in  
39  
40 sample solutions. (B) Anodic stripping voltammograms of the deposition electrode after  
41  
42 377  
43  
44 378 observing the deposition current shown in Fig. A.  
45

46 379

47  
48  
49 380 **Figure 4.** (A) Anodic stripping voltammograms obtained with the deposition electrode  
50  
51 on the chip device after 60 min of deposition with endotoxin concentrations of 0, 0.5, 1,  
52  
53 381  
54  
55 382 10, 100 and 1000 EU L<sup>-1</sup>. (B) Calibration curves for quantitative detection of  
56  
57  
58  
59  
60



1  
2  
3  
4  
5  
6 383 SSV-based electrochemical assay with the chip device. Electrical charges calculated  
7  
8  
9 384 from the voltammograms of ASV are plotted versus endotoxin concentration. Error bars  
10  
11  
12 385 indicate  $\pm$ standard deviations ( $n = 3-6$ ).  
13  
14  
15  
16  
17  
18  
19  
20  
21  
22  
23  
24  
25  
26  
27  
28  
29  
30  
31  
32  
33  
34  
35  
36  
37  
38  
39  
40  
41  
42  
43  
44  
45  
46  
47  
48  
49  
50  
51  
52  
53  
54  
55  
56  
57  
58  
59  
60

1  
2  
3  
4  
5  
6  
7  
8  
9  
10  
11  
12  
13  
14  
15  
16  
17  
18  
19  
20  
21  
22  
23  
24  
25  
26  
27  
28  
29  
30  
31  
32  
33  
34  
35  
36  
37  
38  
39  
40  
41  
42  
43

Fig. 1

A

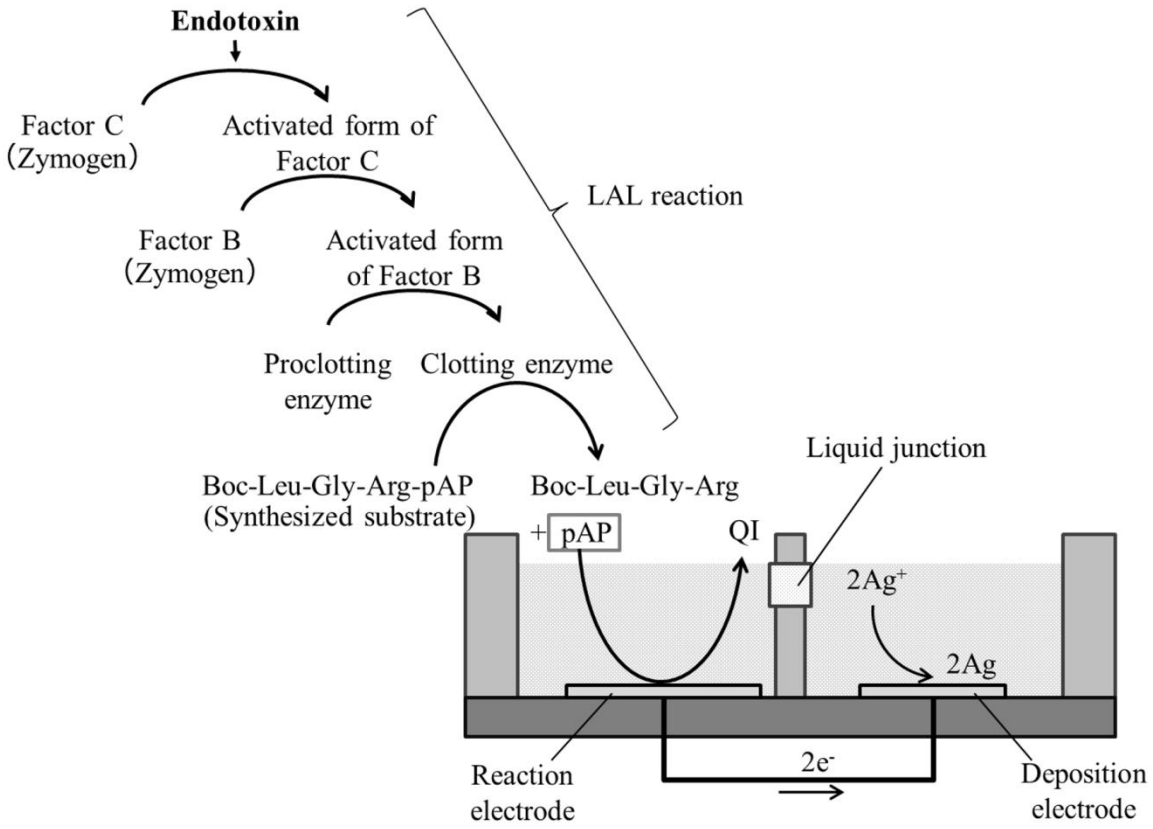
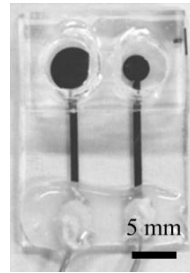
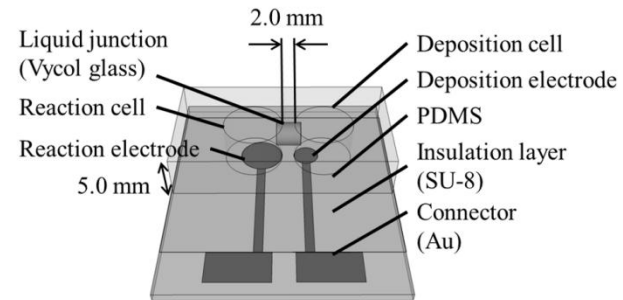


Fig. 1 (Continued)

B



C



1  
2  
3  
4  
5  
6  
7  
8  
9  
10  
11  
12  
13  
14  
15  
16  
17  
18  
19  
20  
21  
22  
23  
24  
25  
26  
27  
28  
29  
30  
31  
32  
33  
34  
35  
36  
37  
38  
39  
40  
41  
42  
43

Fig. 2

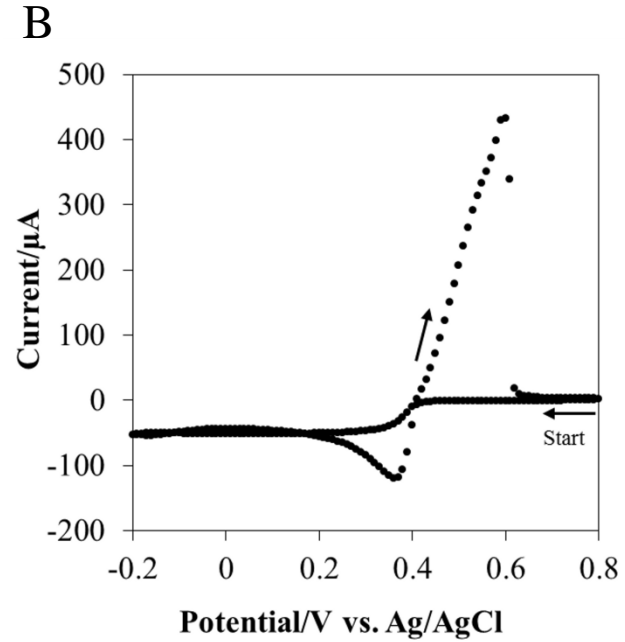
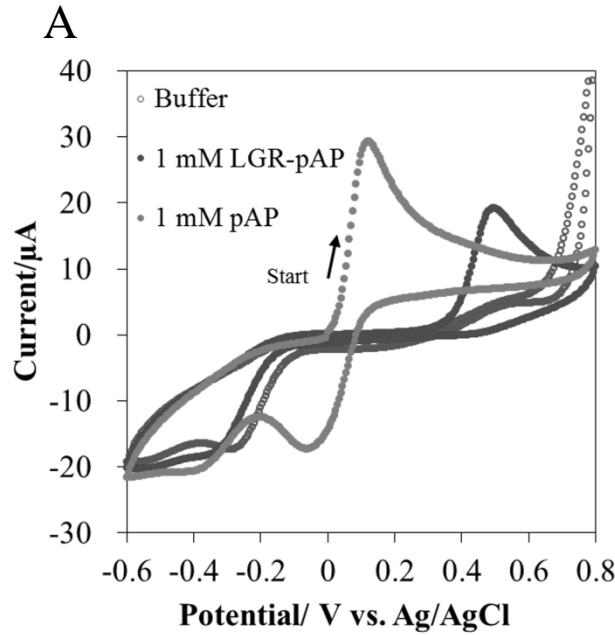
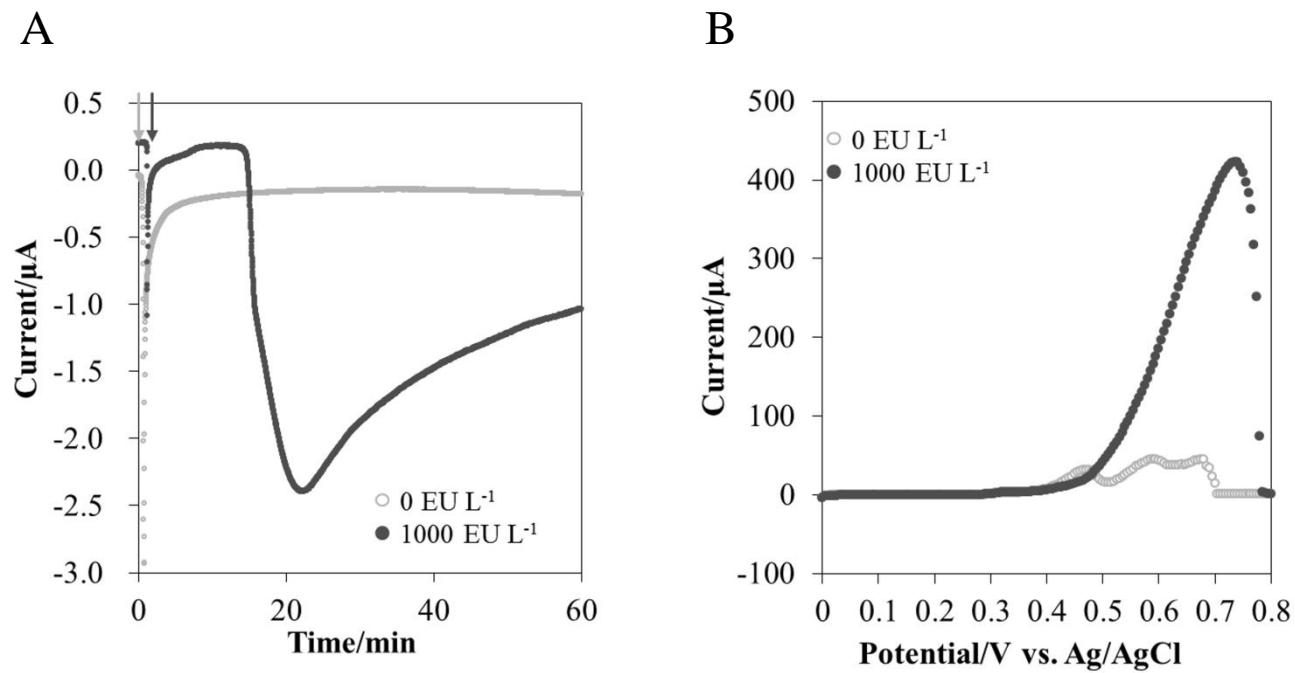


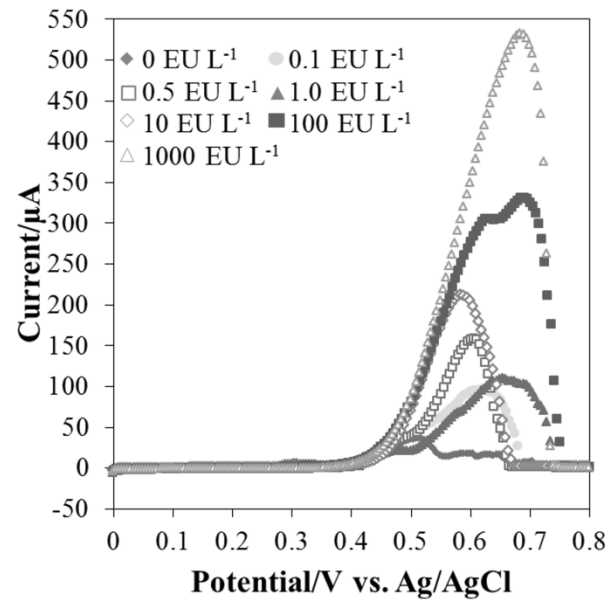
Fig. 3



1  
2  
3  
4  
5  
6  
7  
8  
9  
10  
11  
12  
13  
14  
15  
16  
17  
18  
19  
20  
21  
22  
23  
24  
25  
26  
27  
28  
29  
30  
31  
32  
33  
34  
35  
36  
37  
38  
39  
40  
41  
42  
43

Fig. 4

A



B

